



CELLULAR GROWTH OF A DILUTE BINARY ALLOY AT HIGH SOLIDIFICATION VELOCITIES

A. Ludwig

Giesserei-Institut, Rheinisch-Westfälische Technische Hochschule Aachen
D-52056 Aachen, Germany, E-mail: ludwig@gi.rwth-aachen.de

W. Kurz

Laboratoire de Métallurgie Physique, École Polytechnique Fédérale de Lausanne (EPFL)
CH-1015 Lausanne, Switzerland, E-mail: kurz@dmx.epfl.ch

(Received March 11, 1996)

(Accepted June 25, 1996)

Introduction

In directional solidification of binary alloys at given temperature gradient, the interface morphology changes with increasing growth rate V from (i) planar to cellular, (ii) cellular to dendritic, (iii) dendritic to cellular and (iv) cellular to planar [1]. The critical velocities for the transitions (i) and (ii) increase with decreasing alloy concentration, whereas for the transitions (iii) and (iv) they decrease. Therefore the velocity range for the dendritic growth diminishes with decreasing concentration, resulting in a critical concentration C_0^d below which dendritic growth disappears. A similar decrease of the velocity interval, where cellular growth occurs, appears by further reduction of the alloy concentration. The boundary between planar growth and cellular front is defined by stability theory [2-5]. Below the limiting point (C_0^*, V^*) of the neutral stability curve it was predicted that the planar interface morphology is stable. This prediction has recently been observed in transparent organic alloys by the authors [6].

In this paper experimental studies of the cellular growth morphology near the limit point (C_0^*, V^*) of the neutral stability curve and below the critical concentration C_0^d for the appearance of dendritic growth patterns are presented.

Experimental Procedure

In situ observations of the interface morphologies in the SCN-Argon system were performed by rapidly pulling long, fine capillary tubes, from a furnace into a liquid coolant. The capillaries, used in this work, had a inner cross section of $200 \times 200 \mu\text{m}^2$ with a wall thickness of $100 \mu\text{m}$. They were 900 mm long and made of borosilicate glass. They were filled with SCN-Ar alloys, which had a liquidus-solidus interval between $\Delta T_0 = 60 \pm 40 \text{ mK}$ and $\Delta T_0 = 970 \pm 70 \text{ mK}$. Details concerning the purification of the SCN can be found in [7] and concerning the alloying, the filling procedure and the measuring of ΔT_0 can be found in [6].

The apparatus used in the experiments consisted of a long furnace, a cooling chamber where the liquid coolant was pumped through, and a pulling device, which permitted pulling velocities between 1 and 30 mm/s to be achieved. For a solidification experiment the capillary tube was first threaded through the seals of the cooling system. After the walls of the tube were aligned parallel/perpendicular to the optical axis of the microscope, the tube was moved with constant velocity from the furnace into the coolant.

The solidification front was observed through the coolant, perpendicularly to the solid-liquid interface, and simultaneously, from the side with an optical microscope. Local solidification velocities V (normal to the solid-liquid interface) between 0.3 mm/s and almost 2 mm/s could be achieved. Further details on the experimental procedure and the material properties of the SCN-Ar system are given in [6].

Results and Discussion

The solidification within the square cross section tubes took place almost perpendicular to the walls. The first solid was formed as flat surface dendrites, within one or several edges of the tube. The surface dendrites, with their typical doublet-tips, are the subject of another paper [8]. Beyond the lateral impingement of the surface dendrites, the solid-liquid interface took the form of a pyramid. Apart from the tip and the root region of the pyramid, the four solidification fronts were approximately flat and nearly parallel to the glass walls. Thus the solidification process in this region normal to the glass wall could be regarded as being at steady state.

The solidification microstructure could be observed from a top as well as from the side in projection. Figure 1 shows such views of cellular interface morphologies of SCN-Ar alloys with $\Delta T_0 = 480 \pm 40$ mK and with $\Delta T_0 = 970 \pm 70$ mK for two different solidification velocities. The microscope was focused on the bottom plane of the pyramidal interface. Although the depth of focus was limited, the cellular morphology is also visible at the sides. The distance between opposite interfaces in figure 1 is between 70 μm and 100 μm , which is typical for the observation window used in the experiments. The dependence of the cell spacing, λ , on ΔT_0 can hardly be seen, whereas the velocity dependence is obvious. For the cell amplitude, l , the dependence on ΔT_0 and V is more pronounced. The dark shadow in figure 1b indicated an air bubble in the coolant, which caused a fluctuation in the cooling condition. The resulting variation in the growth rate (see left interface boundary in fig. 1b) is the reason for the large error in the estimation of V , which is one order of magnitude larger than usual.

With the assumption that the solidification conditions at the different planes of the pyramidal interface were comparable and that the crystal growth was perpendicular to the solid-liquid interface, the actual growth rate could be calculated from the angle α between the normal to the interface and the axis of the tube, by $V = V_0 \cdot \cos\alpha$ with actual pulling speed V_0 . Due to changes in the glass wall thickness or to the internal width of the tube, the cooling conditions sometimes fluctuated slightly during an experimental run. Thus the angle α revealed small variations. To obtain an average value of α , five different images in direct chronological order were evaluated. Mean values were obtained by measuring the angle of the two visible interface slopes in one image, each angle measured twice, and taking the average. From the average values of the five images a main average value was calculated. The standard deviation of this averaging was taken as the measuring error for α . Because the pulling speed could be estimated much more precisely, the relative error of V was assessable by the relative error of α . Usually the measuring error for V was smaller than ± 0.07 mm/s.

It was found, that reducing the solute content, i.e. the liquidus-solidus interval, from $\Delta T_0 = 435$ mK to $\Delta T_0 = 60$ mK resulted in a morphological transition from circular cells to a planar growth front [6]. Above $\Delta T_0 \geq 435$ mK, circular cells were observed. These are indicated by the filled markers in figure

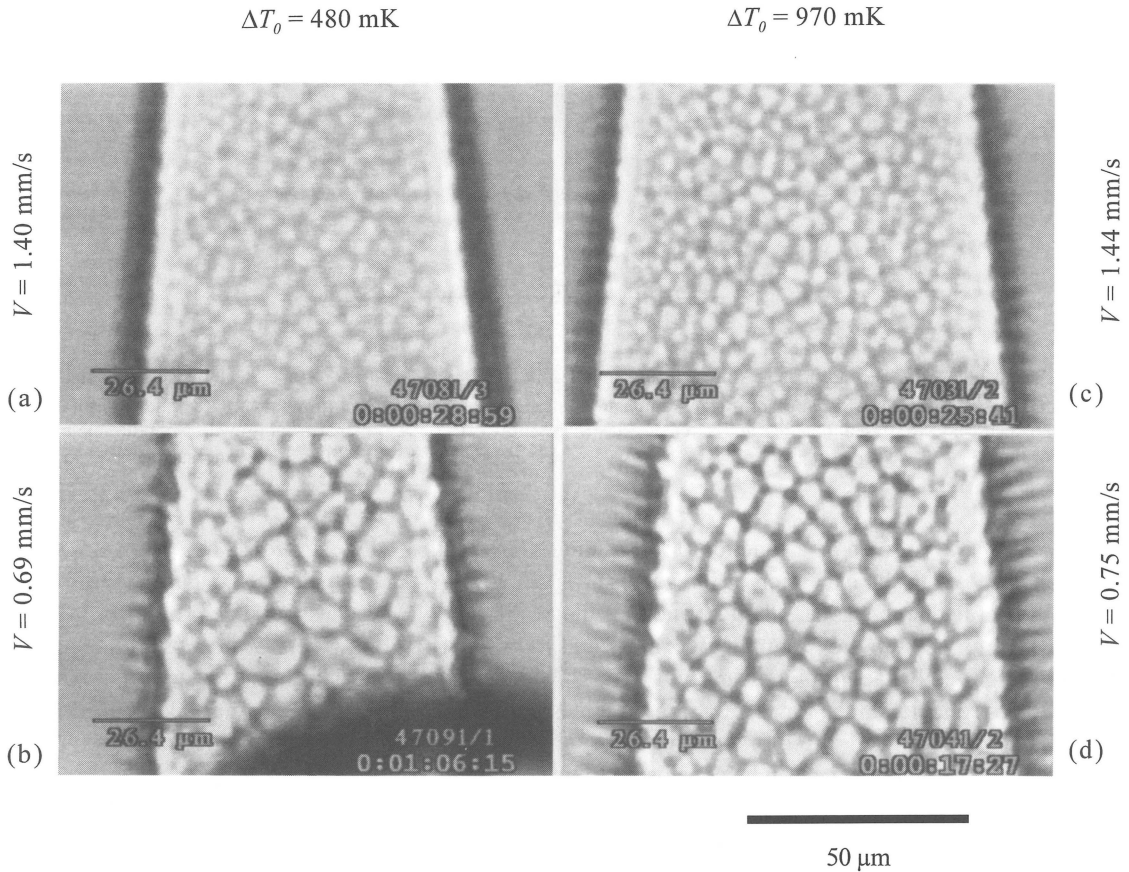


Figure 1. Cellular interface morphology for a dilute SCN-Ar alloy with $\Delta T_0 = 480 \pm 40$ mK for (a) $V = 1.40 \pm 0.06$ mm/s and (b) $V = 0.69 \pm 0.4$ mm/s and a more concentrated one with $\Delta T_0 = 970 \pm 70$ mK for (c) $V = 1.44 \pm 0.03$ mm/s and (d) $V = 0.75 \pm 0.05$ mm/s.

2, where the transition from cellular to planar front growth is shown. The curve represents neutral stability for $G_L = 5 \times 10^4$ K/m, $D = 6 \times 10^{-8}$ m²/s, $k = 0.2$, where G_L is the temperature gradient in the liquid normal to the interface, D diffusion coefficient in the melt, k equilibrium distribution coefficient. Details on the calculation of the neutral stability curve are given in [6]. The critical concentration C_0^d , namely the critical liquidus-solidus interval ΔT_0^d , for the appearance of dendrites, assuming $G_L = 5 \times 10^4$ K/m, is in the order of $\Delta T_0^d = 2.3$ K [9].

The cell spacing was measured by counting the numbers of cells in a defined area and calculating the equivalent average radius [10]. For the measurement of the cell amplitudes, two lines were drawn parallel to a side view of the interface, one connected the cell tips and the other to the extreme values of the cell tails. The distance between the two lines was taken as cell amplitude. The estimation of the average cell spacing, λ , and the average cell amplitude, l , was performed on the same images as for the evaluation of α . From these five λ - or l - values an average value was calculated. The standard deviation of this averaging was taken as measuring error for λ and l , respectively.

With increasing distance from the cell tips, the cell walls became less and less well-defined. Therefore the cell amplitude might be larger than the measurements presented here. This unknown offset is expected to be independent of ΔT_0 and V .

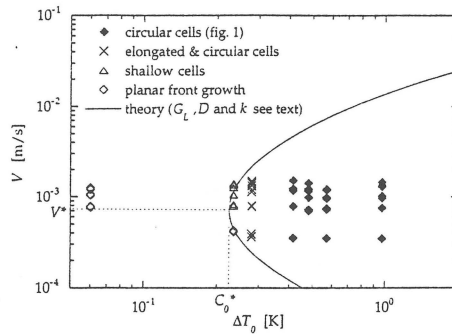


Figure 2. The cellular interface morphologies investigated in this work (filled markers: \blacklozenge) are located within the neutral stability curve (line) close to the "nose". The other markers indicate the transition to planar front growth: (X) a cellular morphology where elongated cells are present together with circular cells, (\triangle) shallow cells and (\diamond) planar front growth. Note that the measuring error for ΔT_0 is in the order of ± 40 mK for $\Delta T_0 \leq 480$ mK and ± 70 mK for $\Delta T_0 = 970$ mK. The measuring error for V is usually smaller than ± 0.07 mm/s.

In figure 3a, λ is given as a function of V for the different alloy concentrations. The error in λ was less than $\pm 5\%$, with the exception of the values at $V \leq 0.4$ mm/s. At low velocity the numbers of cells within the defined area was less than 20 and thus the evaluation of λ was less reliable. The error in V is about ± 0.07 mm/s (with the exception of V measured from fig. 1b). For a given V , the more dilute alloy revealed larger cell spacing. A power law fit, $\lambda^a \cdot V = \text{const.}$, to the measuring point (with the exception of the unreliable values for $V \leq 0.4$ mm/s) gives the following exponent on λ : $a = 1.51$ for $\Delta T_0 = 480$ mK, $a = 1.47$ for $\Delta T_0 = 570$ mK and $a = 1.43$ for $\Delta T_0 = 970$ mK. Within the uncertainties of the measurements the exponent a can be considered to be constant and close to 1.5.

Approximating the thermal gradient within the liquid with $G_L \approx 5 \times 10^4$ K/m and considering the energy balance for a flat interface reveal that the thermal gradient in the solid is of the order of $G_S \approx 10^5$ K/m for $V = 0.5$ mm/s and $G_S \approx 3 \times 10^5$ K/m for $V = 1.5$ mm/s. Although this approximation is strictly valid only for a flat interface, a similar variation of the thermal gradient across the cellular interface with V is also conceivable in our experiments.

Figure 3b shows the dependence of l on V for the same experiments. The measuring error in l was again less than $\pm 5\%$. For the very deep cells the cell tails were located at the boundaries of the images.

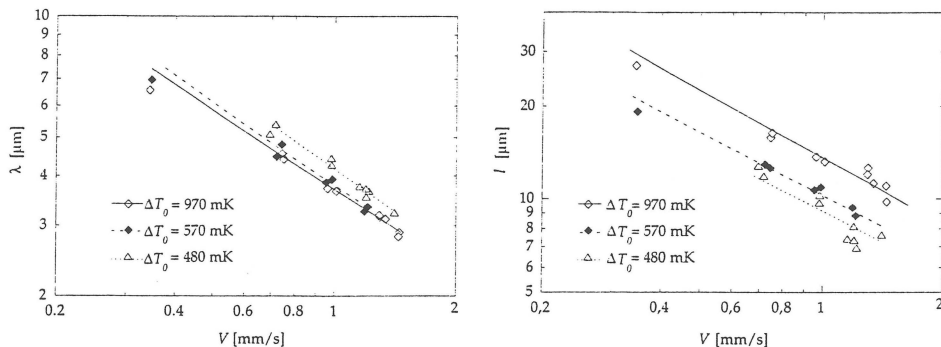


Figure 3. (a) Cell spacing λ as a function of solidification velocity V for the different alloy concentrations. The error in λ is less than $\pm 5\%$, with the exception of the low velocity values (see text). The error in V is about ± 0.07 mm/s (except the value from fig. 1b) (b) Cell amplitude l as a function of V for the same experiments. The error in l is smaller than $\pm 5\%$, but in addition, there might be a further unknown offset (as discussed in the text).

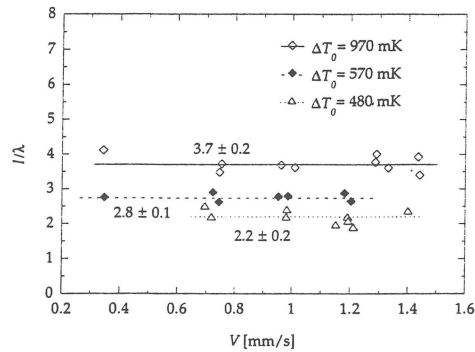


Figure 4. Ratio between cell amplitude l and cell spacing λ as a function of velocity V . Within the investigated velocity range this ratio is independent of V . It decreases with decreasing concentration (i.e. decreasing ΔT_0). The cell amplitude for cells with a ratio smaller than 2.2 could not be measured reliably. Due to the neutral stability curve in Figure 2, the cellular growth at velocities in the order of 1 mm/s will disappear for $\Delta T_0 = 230$ mK.

Thus the estimated values for l must be considered to have a larger error. Approaching V_{abs}^+ , it is obvious that l must decrease with velocity. Because l is correlated with the thermal length, $l_T = \Delta T_0/G$, higher concentrated alloys reveal deeper cells.

The ratio between cell amplitude l and cell spacing λ as a function of velocity V is shown in figure 4. Within the investigated velocity range this ratio is independent of V . It decreases with decreasing ΔT_0 . The cell amplitude with a ratio smaller than 2.2 could not be measured reliably from the images. Due to neutral stability (fig. 2) the cellular growth at velocities in the order of 1 mm/s disappear for $\Delta T_0 = 230$ mK.

Conclusions

Experimental investigations of cellular growth near the limit point of the neutral stability curve reveal the following items:

- (1) In the investigated concentration and velocity range, cell spacing scale with growth velocity by $\lambda^{3/2}V = \text{const}$. A theoretical prediction of a scaling law between l and λ has yet not been given.
- (2) For the investigated low amplitude cells, the relation between cell spacing and cell amplitude is independent of the growth velocity, indicating that l scales with V by the same scaling law than λ .

Acknowledgements

This work was done during a research year of A.L. at the EPFL Lausanne, with grant aid from the Deutsche Forschungsgemeinschaft under Lu 495/2, for which the authors gratefully acknowledge. The valuable help of J. Stramke in preparing the experiments and of P. Gilgien in calculating the cell to dendrite transition is also gratefully acknowledged.

[†]For an alloy with $\Delta T_0=480$ mK and $G_L=5 \times 10^4$ K/m V_{abs} is 5.9 mm/s.

References

1. W. Kurz, D.J. Fisher, Fundamentals of Solidification, Trans Tech, Aedermannsdorf, Switzerland, 3rd edition, 1992.
2. W.W. Mullins, R.F. Sekerka, J. Appl. Phys. **35** (1964) p. 444.
3. S.R. Coriell, R.F. Sekerka, J. Cryst. Growth **61** (1983) p. 499.
4. G.J. Merchant, S.H. Davis, Phys. Rev. B **40** 16 (1989) p. 11 140.
5. D.A. Huntley, S.H. Davis, Acta Metall. **41** (1993) p. 2025.
6. A. Ludwig, W. Kurz, Acta Metall. Mater., accepted for publication.
7. H. Esaka, Sc.D. Thesis, EPFL Lausanne (1986).
8. A. Ludwig, W. Kurz, to be published.
9. ΔT_o^d was calculated by P. Gilgien using a program for cellular and dendritic growth developed by Lu and Hunt (S. Lu, J.D. Hunt, J. Cryst. Growth **123** (1992) p. 17).
10. B. Billia, R. Trivedi in: *Handbook of Crystal Growth*, Vol. 1B, ed D.T.J. Hurle (Elsevier Science Publishers, Holland, 1993) p. 899.